Modeling Low-ID Movement Evaluation of Input Devices in a Ballistic Sketching Task

by

Victor Clifford Alkin Mac Farlane

A thesis submitted to the
Department of Computing and Information Science
in conformity with the requirements for
the degree of Master of Science

Queen's University
Kingston, Ontario, Canada
October 2005

Abstract

Oscillatory movements used in shading, hatching or instrument vibrato play an important role in artistic interactions. They are also becoming more common in modern graphical interfaces, such as the Tablet PC. However, because these movement tasks are ballistic tasks users' performances are not modelled appropriately by current models for movement which apply to pointing tasks.

Previous research into this type of movement has focused on movements using stylus style devices of various weights, and has dealt with movements with larger amplitudes then are found in typical computer interfaces, rather the focus of the research was on tasks which required moving objects up to 36cm distance, which is much larger then movement used to control modern computer devices. We focused our research on movements similar to those found in computer interface controls, where movement is less then 6cm, and in the case of the isometric joystick, there is no movement at all.

In this thesis, we introduce a model for a ballistic line hatching task, which provides us with an experimental paradigm to investigate the Oscillatory movements used in shading, sketching and vibrato. We constructed an experiment to model line shading using an isometric joystick, mouse and stylus. We found that a simple sketching law does indeed exist. Our results showed a good fit with the model, with

correlation coefficients of 0.89, 0.96,and 0.96 for the isometric joystick, mouse and stylus respectively.

Acknowledgments

I would like to thank...

Contents

List of Tables

List of Figures

Chapter 1

Introduction

1.1 Fitts' Law

The modeling of pointing behavior has been of great value in evaluating the efficiency graphical user interfaces. This understanding allows the designer to do a numerical evaluation of a prospective design. These models of pointing behavior are also unutilized in evaluating the efficiently of input devices such as the mouse or stylus. In the field of Human Computer Interaction the most important of these models, Fitts' law, relates movement time in pointing tasks to the size and distance of the target [20]. This model explains up to 99% of the variance of pointing tasks, making it one of the few mathematical models in HCI that is empirically robust.

Fitts' law is a model of human psychomotor behaviour based on Shannon's Theorem 17, a fundamental theorem of communication systems [5]. Fitts' model is analogous to the transmission of "information" in electronic systems. Movements are assigned an index of difficulty, in "bits", and in carrying out a movement task the

human motor system is said to transmit so many "bits of information". If the number of bits is divided by the time to move, then a rate of transmission in "bits per second" can be determined. Shannon's Theorem 17 expresses the effective information capacity C (in bits/s) of a communications channel of bandwidth B (Hz) with signal power P, and noise N.

$$C = B\ log_2\left(\frac{P+N}{N}\right) \tag{1.1}$$

or

$$C = B\ log_2\left(\frac{P}{N}+1\right) \tag{1.2}$$

Fitts' conducted his investigation of the human motor system using four experiments: two reciprocal tapping tasks (1 oz stylus and 1 lb stylus), a disc transfer task, and a pin transfer task. In the tapping experiments the subjects moved a stylus back and forth between two metal bars as quickly as possible and tapped the bars at their centers (see Figure 1). This experimental arrangement is commonly called the "Fitts' paradigm".

Fitts related the target amplitude of the task, A, to the signal power in Shannon's theorem 1.1, and the target width W to the noise N. Fitts called this value the Index Of Difficultly ID. Fitts asserted that this Index Of Difficulty is equal to the information that is "transmitted" by the human motor system during the task, and this given by equation 1.3

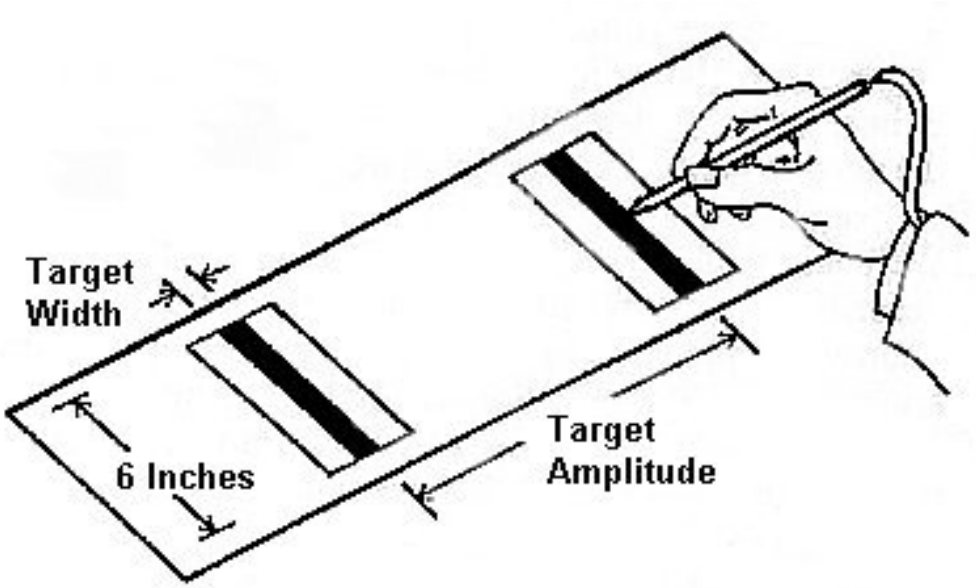

Figure 1.1: The reciprocal tapping paradigm

$$ID = log_2\left(\frac{A}{W}\right) \tag{1.3}$$

Fitts found a very high correlation between Movement Time (MT) and the Index of Difficulty (ID). However, for low IDs (IDs less then 2) the appropriateness of the model is greatly reduced (see Figure 2). It is these low ID movements which are the subject of this thesis.

Note that Fitts' Index of Difficulty equation 1.3 is not in the form of Shannon's theorem 17 1.1. Rather it more closely resembles Goldman's Equation 39 1.4 [12].

$$C = B\ log_2\left(\frac{P}{N}\right) \tag{1.4}$$

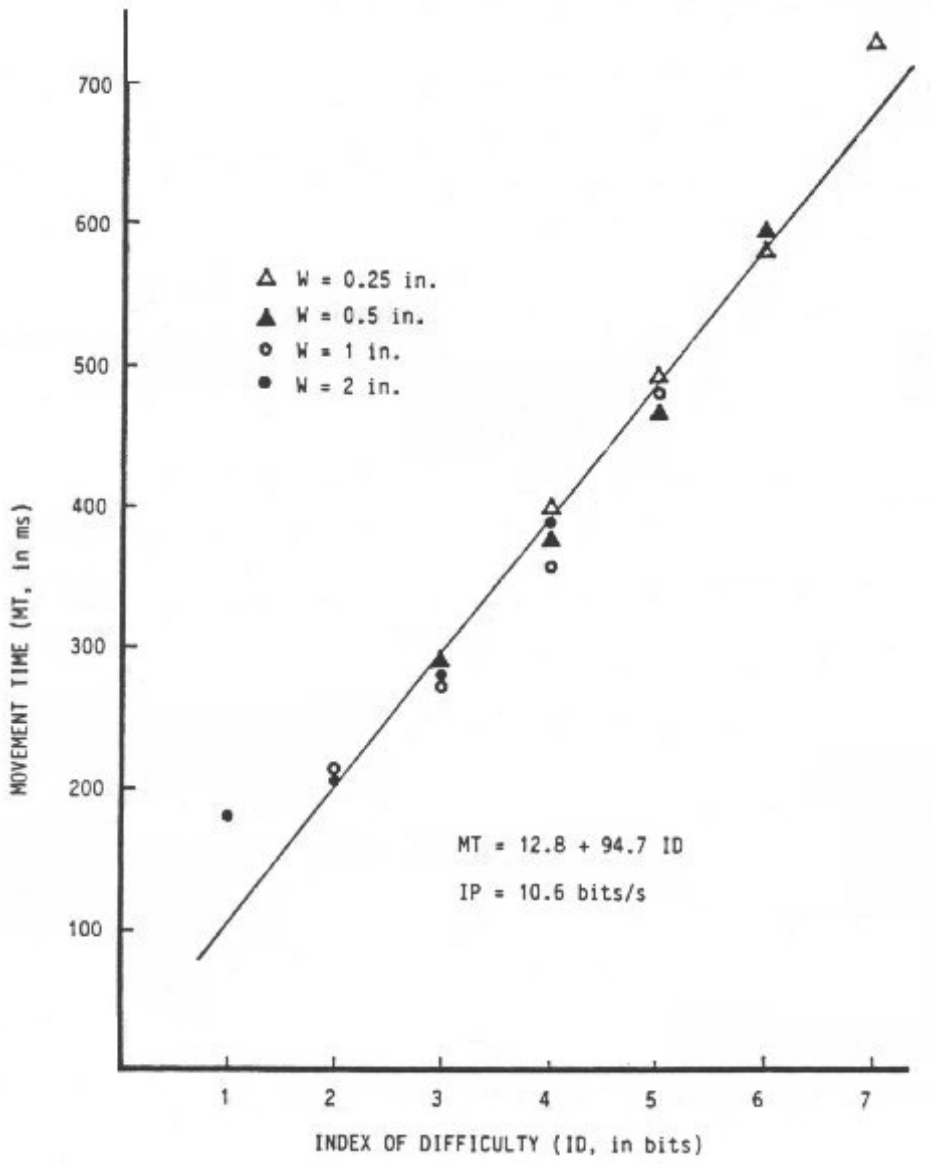

Figure 1.2: Scatter plot

Goldman's equation is approximation of Shannon's Theorem, which is is widely used in communication theory instead of Shannon's Theorem [5]. Goldman's equation is well suited to applications where the signal power is much greater then noise, as it greatly simplifies most calculations. Later research in the field [18] expresses the index of difficulty in a form closer resembling Shannon's Theorem

In its most common form [18], Fitts' law states that the movement time, MT, required to point to a target of width W at a distance A is governed by the following relationship.

$$MT = a + b\ log_2\left(\frac{A}{W} + 1\right) \tag{1.5}$$

where a and b are emprically determined constants. The difficulty of the task, called the Index of Difficulty (ID) is given by the the log term in equation 1.5.

$$ID = log_2\left(\frac{A}{W} + 1\right) \tag{1.6}$$

Since more time is needed to acquire a smaller target or move a larger distance, a larger ID indicates a more difficult task. The index of performance (IP) is given by the reciprocal of b [16], and is indicative of the overall efficiency of the pointing device. This index of performance (IP) is independent of the experimental conditions, allowing researchers to compare performance data for input devices from different studies.

1.2 The Welford Correction

The Welford correction [27] is a method for correcting of errors described by Crossman [8]. It makes use of the fact that the information in a normal distribution is $\log 2\sigma\sqrt{(2\sigma\pi e)}$, where σ is the standard deviation of the distribution. Now $sqrt(2\pi e)$ = 4.133 and a range of +/- half this is, i.e. 2.062σ, includes about 96% of a normal distribution. Welford argues that if about 4% of the shots fall outside of the target, $\log 2$ W, where W is the width of the target, is an accurate representation of the information contained in the distribution of shots.

Welford argues that when errors are greater then 4% then the effective target width is greater then W, and when errors are less then 4% then the effective target width is less then W. Welford proposed estimating the standard deviation σ from the error rate obtained using table for normal distributions. Hence giving an effective target width equal to 4.133 σ. Welford used Fitts's 1968 data and showed a closer fit when effective width was used in the place of width.

Traditionally the Welford correction is used on experimental data, when the error rates exceed 5%. As of the writing of the paper, I was unable to find any papers that calculate the standard deviation directly to determine the effective width.

1.3 Limitations of Fitts' Law

Since early studies comparing the performance of various input devices using IP [6], Fitts' law has been extended to accommodate a more diverse set of tasks, such as two-dimensional target acquisition [17], bivariate pointing [3], and, most importantly, trajectory-based tasks [1]. However, we believe there are still a number of outstanding

issues that limit the ecological validity of Fitts' law with regard to input device evaluations for certain tasks.

Firstly, pointing efficiency is not always indicative of the efficacy with which an underlying task is completed. This is particularly true when the underlying task requires movement that cannot easily be modeled as a simple targeting gesture. A good example of this can be found in line drawing. Here, the time it takes to connect lines is not indicative of the quality of the result. Instead, the specific shape or curvature of the lines may be much more relevant. Such creative tasks are not easily modeled using any of the known variations of Fitts' law.

Secondly, Fitts' law models information processing in closed-loop hand movements. Although there are many control tasks that follow the general model provided by Shannon and Weaver [5], it is important to note that Fitts' law is not appropriate when modelling input device performance in tasks that do not allow for a closed-loop hand-eye coordination process. Examples include ballistic input conditions, where movement is completed before visual feedback can be processed. Evaluating isometric input conditions may also be problematic, as there may be no significant hand movement. Rather than trying to evaluate devices that appear useful for non-pointing tasks with Fitts' law, we believe it would be beneficial if we could model more closely the way in which physical activity relates to task performance. Part of the underlying problem then is to extend or generalize Fitts' law performance of a device to tasks other than pointing.

1.4 Isometric Movement

Isometric Input One of the input devices that, for the above reasons, has perhaps not been fully appreciated in pointing evaluations is the isometric joystick. When isometric joysticks, such as the IBM Trackpoint, are used in pointing tasks, the force exerted on the joystick is typically translated into a rate of position change of the on-screen cursor. Feedback on targeting action is provided by the visual location of the on-screen cursor. When using the mouse, visual feedback corresponds well with kinesthetic feedback on the location of the hand. When using an isometric device, tactile-kinesthetic feedback describes the cursor velocity, rather than its position. This discrepancy may well explain lower Fitts' law performance of isometric devices in pointing tasks. As a result, isometric devices like the Trackpoint are consistently classified as having a lesser index of performance than the mouse [2, 6, 9, 10, 22].

However, we must stress such conclusions pertain only to the use of isometric devices in rate-controlled pointing. It is interesting to note that isometric input is indeed involved in many artistic tasks. For example, most musical instruments incorporate forms of input that can be modelled as isometric. Moreover, such input is used for some of the most time-critical tasks, such as vibrato [24].

We believe this is for three reasons. Firstly, the passive tactile-kinesthetic feedback provided by isometric devices allows one to very tightly control the curvature of parameter movement [7, 24]. Secondly, isometric input is typically applied to control parameter deviation [25], rather than the selection of some absolute parameter value. This facilitates the absolute mapping of force to parameter, enhancing the correspondence between tactile-kinesthetic and visual-auditory feedback on parameter state [19]. Finally, isometric control is fast because there is minimal positioning

of the hand involved [21]. In tasks that involve oscillation around a given absolute value, isometric control may give very high modulation speeds indeed.

An example of such task is vibrato on a string instrument. In vibrato, the pitch of the sound is modulated rapidly relative to a given absolute pitch. The absolute pitch is typically chosen by hand positioning on the string during intonation. Vibrato is then performed by rocking the finger back and forth while pressing the string. This action may be considered isometric, since it involves minimal movement of the finger or hand [24].

1.5 Defining the Task

Based on our design experiences with SensOrg [25], a tangible computer music instrument, we were particularly interested in evaluating performance of input devices in rapid oscillatory tasks. Of the above three arguments, control over the curvature of the movement appeared the most difficult to investigate empirically [7]. Instead, we created an evaluation task that involved high velocity movement relative to a center point. For the purposes of this experiment, we chose a visual control task that modelled an oscillatory task in the following way:

a) It required users to move an on-screen cursor back and forth between two boundary lines visible on the screen;

b) It required little hand movement.

c) It provided no specific target constraints other than having to cross the two boundary lines with minimal overshoot.

The task represented a very common sketching activity shown in Figure 1a: that of line shading an area. Figure 1b shows how we may consider such a task as an

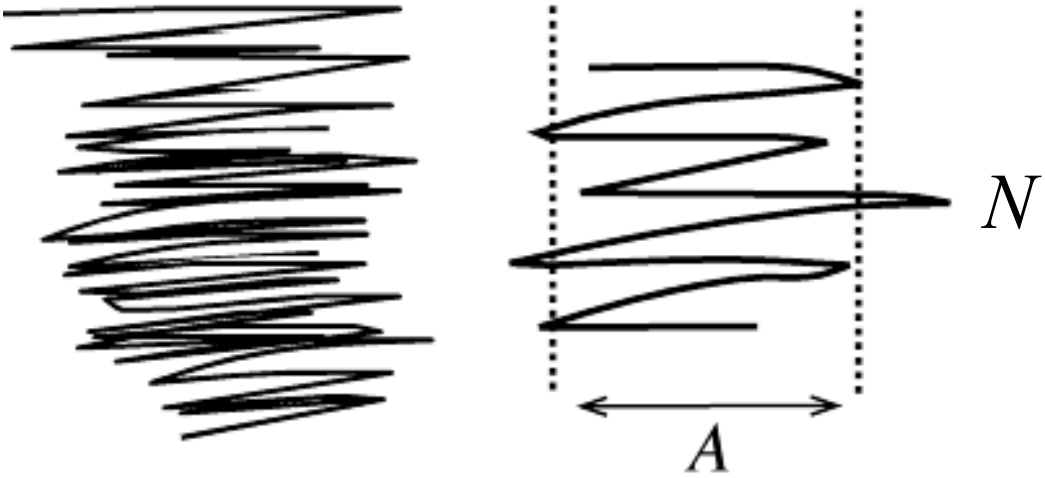

Figure 1.3: Line shading task, and corresponding Model of the task.

oscillating movement between two extremities placed at distance A, where N represents the number of oscillations. The accuracy constraint in this task is relaxed, and consists of crossing the extremities in a way that optimizes speed between crossings. This implies the task has no strict width constraints in terms of Fitts' law. If we assume small amplitudes, we may consider the task to involve little hand movement, and therefore to be well-suited to isometric control. Moreover, an absolute mapping of force to cursor location could be facilitated in this task by considering the center between the two lines as a zero or null location. In this paper, we discuss our investigation of the efficiency of three input devices in this task: the Wacom stylus, a Logitech optical mouse and a high-resolution analog isometric joystick based on Clynes' original Sentograph [7]. We expected the isometric joystick to outperform mouse and stylus in this task.

1.6 Literature Overview

In classic Fitts' law studies, isotonic devices such as the mouse typically outperform isometric joysticks. Performance of isometric devices does follow Fitts' law, in that models provide a tight fit with empirical observations [6, 4, 22]. One of the first studies to show inferior performance of isometric input was by Card et. al. [6]. Subsequent studies replicated those results, confirming superiority of the mouse and stylus in terms of speed and accuracy. [2, 9, 10, 22]. To the best of our knowledge, the majority of studies evaluating isometric input employed a rate-controlled cursor mapping. Interestingly, a study by Kantowitz and Elvers [4] found that position-controlled isometric joysticks yielded higher performance than rate-controlled isometric joysticks in Fitts' law tasks. Mithal and Douglas [19] investigated the differences in performance between the rate-controlled isometric joystick and mouse by looking at the microstructure of movement with the devices. By inspecting graphs of cursor velocity against displacement, they found that the joystick amplified physiological tremor in the finger. This tremor caused random and involuntary variations in the velocity which made the joystick more difficult to control. They concluded this tremor might be the cause of the poor performance in pointing experiments, where a fine degree of control and accuracy is required. Zhai and Milgram [23] suggested that the lack of correspondence between proprioception and exteroception may make it more difficult to learn a pointing task using an isometric device with a rate-controlled mapping. However, their experiment did not show a negative overall performance impact after practice.

1.7 Modeling Low-ID Movement

Modeling Low-ID Movement According to Gan and Hoffmann [11, 14], target acquisition becomes essentially ballistic with movement times below approximately 200 ms. Here, movements are too fast to allow for visual feedback or correction during the task. Since kinesthetic feedback dominates performance in such cases, one would expect an advantage for isometric devices. However, this is only true if a good correspondence between tactile-kinesthetic feedback and parameter feedback is provided. Welford [27] reported non-linearities in the low ID domain of Fitts' law models. Citing Crossman [8], he described a method for adjusting the input data to reflect the actual accuracy, or effective width (We), with which subjects hit a Fitts' law target. He showed that by recalculating regressions using effective width data, a better fit is obtained. Similarly, Gan and Hoffmann [11, 14] investigated what geometric conditions allow a movement to become ballistic. They found that for low-ID conditions, where the ID was below 3.0, movement time was related only to A and not to ID. They opposed Welford's suggestions, arguing instead that the low-ID region of the task is inherently ballistic.

1.8 Model Derivation

Gan and Hofmann proposed an alternate model for ballistic movement tasks. Their model is based on rapid arm movements pivoted around the elbow. According to them, the acceleration of the arm as a function of time approximates a sine curve see equation 1.7, the corresponding torque exerted on the limb is given by equation 1.8. Note that we corrected this from the original to accommodate the fact that movement

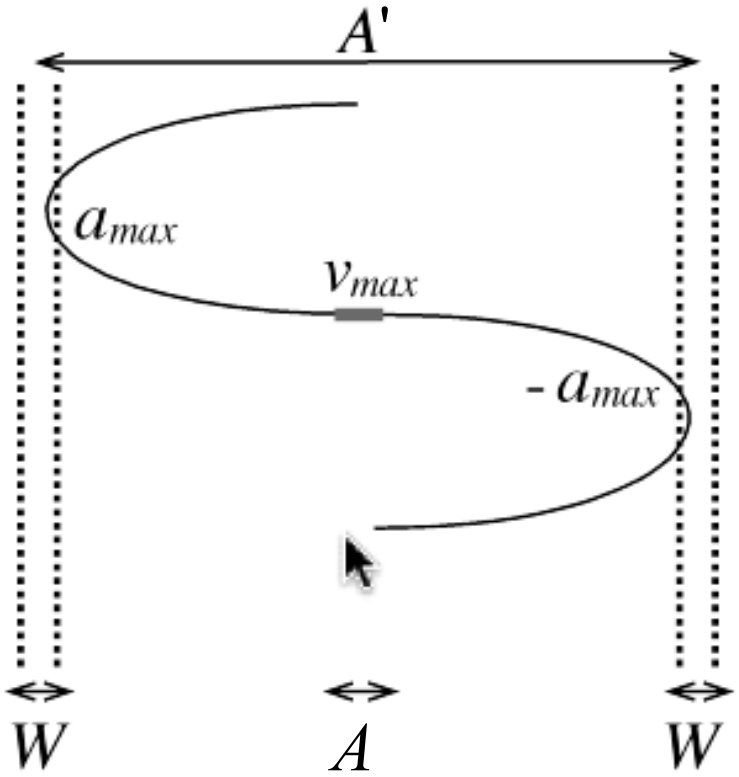

Figure 1.4: Gan and Hoffmann's sine approximation, featuring continuous acceleration or deceleration

time is only half the period). Here, I_a is the moment of inertia of the arm about the axis of rotation and $\ddot{\theta}_{max}$ is the maximum (angular) acceleration of the arm.

$$\alpha = \ddot{\theta}_{max} sin\left(\frac{\pi t}{MT}\right) \tag{1.7}$$

$$Torque(T) = I_a \ddot{\theta}_{max} sin\left(\frac{\pi t}{MT}\right) \tag{1.8}$$

Figure 1.8 shows the corresponding movement pattern, with the arm always either accelerating or decelerating towards the target. Double integration of Equation 1.7

and solving for MT yields the relationship between movement time and amplitude for this movement, which is given by Equation 1.9, which we simplified from [14] and corrected by including an extra factor π. Here, A' is the effective amplitude of the actual distance travelled by the hand (see Fig. 2), I_a is the moment of inertia of the arm, l is the length of the arm, T_{max} is maximum torque, $\ddot{\theta}_{max}$ is the maximum angular acceleration reached during movement, and c is some constant:

$$MT = \sqrt{\frac{\pi^2(A'/2)}{lT_{max}/I_a}} = \sqrt{\frac{\pi^2(A'/2)}{l\ddot{\theta}_{max}}} = c\sqrt{A'} \tag{1.9}$$

Gan and Hoffmann's observations of ballistic hand movements closely followed this model [13, 14, 11]. Gan and Hofmann's model assumes a simple harmonic motion for ballistic hand movements, one in which the maximum acceleration ($\ddot{\theta}$) is the same for all amplitudes. To explain this, a typical form of harmonic motion is given in Equation 4, Hooke's Law. Here a(t) is the acceleration at time t, x(t) the distance from equilibrium (the center of the movement amplitude) at time t, and k is a constant which is typically referred to as the spring constant. Note that here, as in the rest of this paper when we refer to acceleration (a), we are talking about relative acceleration not angular acceleration (α).

$$a = l\ddot{\theta} \tag{1.10}$$

Where a is the relative acceleration at the end of arm, $\ddot{\theta}$ is the angular acceleration, and l is the length of the arm.

$$a(t) = -kx(t) \tag{1.11}$$

From Equation 1.11 one can derive expressions for a(t) (Equation 1.12) and x(t) (Equation 1.13. Here, A' is the effective amplitude of hand motion, thus the amplitude of the sin wave for position is A'/2, recall movement time MT denotes one half period of motion.

$$a(t) = -k\frac{A'}{2}sin\frac{\pi t}{MT} \tag{1.12}$$

$$a(t) = \frac{A'}{2}sin\frac{\pi t}{MT} \tag{1.13}$$

By double integrating Equation 1.13, and comparing the result to Equation 5, we can express the spring constant k in terms of MT:

$$k = \frac{\pi^2}{MT^2} or MT = \frac{\pi}{\sqrt{k}} \tag{1.14}$$

This shows that the movement time for any harmonic motion is dependent on the spring constant (assuming a constant inertia and arm length). A spring with a small spring constant requires less energy to be displaced from center than one with a large spring constant. The tighter the spring, the smaller the period and movement time over a particular amplitude. Gan and Hoffmann's model assumed that k can always be adjusted such that the same maximum acceleration can be achieved for all amplitudes.

In [11] Gan and Hoffmann conducted an experiment in which subjects were asked to move a stylus from a starting plate to a target plate, in this experiment the plate width was varied with the amplitude between the plates to produce a constant 3.0 index of difficulty as computed by the experimenters. Gan and Hoffmann used the following formula for index of difficulty.

$$ID = log_2(\frac{2A}{W}) \tag{1.15}$$

here A is the distance travelled during the movement and W is the width of target. meaning the width of the target plate was approximately the amplitude of the movement divided by four. Each subject was required to carry out ten repetitions of

each of the 120 experimental conditions involving eight directions, three transported masses (0.0, 1.5 and 3.0 for males and 0.0, 0.7 and 1.5 for females), and five amplitudes (4cm, 9cm, 16cm, 25cm and 36cm). Their results showed a strong fit to the square-root model for movement. However, their smallest amplitude was four centimeters. Which is much larger then the typical movements used with modern computers. Also in this experiment the transported masses were weights that were placed on the wrist and participants completed the task by moving their elbow and shoulder. The movements which are the focus of this paper are primarily wrist movements. Also we would suggest that the target size was to small for the movement to be truly ballistic.

1.9 Modeling the Hatching Task

Gan and Hoffmann used a standard Fitts' Law paradigm in their experiments, one with clearly defined target widths. Such paradigm does not appropriately model the Hatching task described in Figure 1, where there are no clear target widths. In a Hatching task, the only constraints are two target lines at amplitude A from one another, which need to be crossed back and forth with as little overshoot as possible (see Figure 1.5). To achieve such movement, the hand-arm motion would perform as a tight spring for small amplitudes, and as a loose spring for large amplitudes, resulting in a harmonic motion path. Without the presence of accuracy constraints, movement will likely be faster than reported in ballistic Fitts' Law experiments, but this also means that the maximum acceleration of the hand-arm system will come close to the limits of the human muscle-skeletal system. As such, we expect limitations in the stiffness (or spring constant) of the hand-arm system to come into play. In [15], Lin et al. assert that apart from limits to the acceleration of the arm, which were discussed

by Gan and Hoffmann, there is also a maximum value to the stiffness of the hand-arm system. While no clear values were given, stiffness depends on which muscle groups are being used. The stiffness of the hand-arm system is analogous to the spring constant k (note that the use of the word constant is somewhat confusing as k may actually be variable). From Equation 1.11, we can derive the following relationship between effective amplitude A', the maximum acceleration obtained a_{max}, and the spring constant k:

$$a_{max} = k\frac{A'}{2} \tag{1.16}$$

To achieve the same maximum acceleration at small amplitudes, a large value of k is required. As such, given an upper limit to k, the maximum acceleration may not be reached at small amplitudes. If the upper limit to k is indeed reached, we predict larger movement times for smaller amplitudes then those given by Gan and Hoffmann's square root model (Equation 1.9). The result of this is that the relationship between movement time MT and amplitude A' should be close to some linear equation:

$$MT = a + bA' \tag{1.17}$$

Note that up to this point we have expressed movement time in terms of the actual or effective amplitude A' traveled by the hand. If we can assume that the relationship between target amplitude presented during an experiment is linear with the actual amplitude traveled, we can derive Equation 1.18, which represents our simple Hatching law model:

$$MT = a + bA \tag{1.18}$$

Looking back at the movement represented in Figure 1.5, Equation 1.18 describes a single crossing between two lines at distance A, where a and b are empirically

derived constants (and are different from the constants in Equation 1.17). The index of performance for such model would be the reciprocal of b, and equal to a theoretical maximum velocity (v_{max}). Note that the above model is one-dimensional, and ignores the strokes down the tunnel shown in Figure 1.5. Multiplication by number of strokes N would yield some prediction of the overall movement time for the hatching task depicted in Figure 1.5, but would still not account for movement along the tunnel. We will ignore N for now, focusing instead on empirically establishing whether there is indeed a linear relationship between movement time and target amplitude A, as well as effective amplitude A'. Next, we will discuss how we evaluated the performance of mouse, stylus and an isometric joystick in our Hatching task.

Chapter 2

Research Design

The genesis of this work was an experiment to investigate the efficiency of devices for ballistic low ID movements. Our primary focus was to compare the mouse style and isometric joystick for these tasks. Previous literature on this subject dealt primary with moving stylus style devices of various weights. As stated earlier in the introduction, Previous research in [14, 11, 13] showed that the motion of the human motor system for this task is harmonic in nature, and limited by the maximum torque that can be exerted on the limb, as well the movement time for the task, which we equate to the inverse of efficiency, is was linear with the square root of the distance travelled. The primary focus of this paper, was to compare the isometric joystick with the mouse and stylus for this task. Since the isometric joystick requires no actual movement it was expected that it would not be subject to the same limitations of the stylus and mouse.

The result of this experiment seemed to be in direct contradiction to the previous research in the field [14, 11, 13]. Regression showed a strong fit to a linear model, and a weak fit to the square root model which was supported by Gan and Hoffmann's,

and by Guiard's results.

Farther experiments, and research were done to determine the underlying nature of the movement and to explain why we found a linear relationship, where other researchers found a square root relationship.

Chapter 3

Experiment Implementation

3.1 Experimental Task

3.1 shows our experimental task, as experienced by the participants. The task was to successfully cross two vertical lines on the screen, placed at amplitude A apart, for 25 times. To provide visual feedback on each successful line crossing (useful only during training), the new goal line was painted green, while the old goal line would turn black. All erroneous crossings, where participants crossed the same line consecutively, were dropped from analysis. We used 31 amplitudes evenly spread from 0 (where participants iteratively crossed a single line), to 480 pixels on screen. The order of presentation of devices was controlled using a randomized Latin Square design, with each order done at least once, and no order performed more than twice by each participant. The order of the amplitude presentation was fully randomized, as was the choice of starting target line. Participants trained using a set of 4 amplitudes: 0, 160, 320, and 480 pixels with each device, requiring them to perform a minimum of 50 successful crossings. Participants were required to continue training until their

Figure 3.1: Screenshot of line crossing task as experienced by participants.

crossing time changed less than 10% while maintaining an error rate of less than 5% over their last 3 trials. Most participants placed their wrist on the desk while performing the task, except when using the isometric joystick. Participants were instructed to perform the task as quickly as they could, while minimizing overshoot when crossing the lines. We employed a within-subject design with two factors: input device and amplitude. Our dependent variable was movement time.

3.2 Participants

Participants 11 volunteers, 10 males, 1 female, participated in the experiment. 10 participants were right-handed and 1 was left-handed. Participants used the input devices with their preferred hand. All participants were expert mouse users prior

to the study. 9 participants had some experience with an isometric joystick and 6 participants had some experience with a tablet stylus.

3.3 Apparatus

Apparatus The experiment was conducted on a Dell Dimension 8200 computer running Windows-XP Professional. The machine's 17" LCD display was used at a resolution of 1280 pixels by 1024 pixels. The experiment was conducted in full-screen mode. The mouse used was a Logitech OEM FirstMouse. We used a high-resolution analog 3D joystick design based on Clynes' original Sentograph [7] (shown in 5.7). We only used the x and y torque signals from this joystick. The analog signals from this joystick were converted into USB signals using a Phidget A/D converter [16]. The joystick used an absolute force-to-position transfer function, described in more detail below. The graphics tablet used was a Wacom Intuos 2 [26] (model XD-0912-U, 30.4 cm x 45.7 cm active area, 2540 lpi resolution).

3.4 Device Transfer Functions

The tablet area was mapped to the screen area using a linear absolute mapping. Isometric Joystick Transfer Function Cursor acceleration was turned off for all input devices. To improve the resolution of measurement in pixels during these high-speed movements, the control-to-display ratio was set at 1: 2.2 cm for all positioning devices, rather than the regular 1:1 ratio. 1 cm of mouse movement in the real world corresponded to 80 pixels of cursor displacement.

For convenience, all target amplitudes in our task and results will be reported

in pixels. We did not correct for differences in mass between the mouse and the stylus, as we considered these differences to be inherent to the devices. We did ensure that the amount of force needed to move the cursor was approximately equal for the mouse and isometric joystick. Our joystick control software polled the Phidget driver directly. This reported a value of -720 to +720 across the range of the joystick's force curve, from -3N to +3N of torque. We mapped the x,y force measurements directly to cursor position relative to a 0 location in the center of the screen at 0N of torque. We then calibrated the joystick to move the cursor to the maximum positive amplitude of 240 pixels in our task by applying a force of 1 N and the maximum negative amplitude of -240 pixels in our task by applying a force of -1 N to its tip. This force is approximately equivalent to the force required to move a mouse with a mass of 100 g over the same distance (i.e., 3 cm in real world hand movement).

Chapter 4

Research Results

4.1 Results

Device	$\overline{MT}(s)$	Regression Coefficients			IP(m/s)
	s.e	r^2	a (s)	b (s/m)	
Stylus	0.102	0.96	0.08	0.54	1.84
	0.002				
Mouse	0.120	0.96	0.09	0.86	1.16
	0.003				
Isometric Joystick	0.095	0.89	0.09	0.33	3.01
	0.002				

Table 4.1: Mean movement times, standard errors and Hatching law models for each device. Predicted equations are of the form MT=a + bA, where A represents target amplitude.

Target Amplitude (pixels)	Mouse		Stylus		TrackPoint	
	$\overline{A'}$ (pixels)	$\overline{MT}$ (ms)	$\overline{A'}$ (pixels)	$\overline{MT}$ (ms)	$\overline{A'}$ (pixels)	$\overline{MT}$ (ms)
0	118	93	135	83	315	83
16	114	93	131	83	270	82
32	147	95	169	88	340	87
48	178	101	218	89	352	87
64	192	101	217	91	335	87
80	209	96	240	95	407	88
96	247	103	258	94	381	92
112	275	106	290	96	473	90
128	302	112	313	97	452	90
144	305	110	312	93	457	93
160	331	114	351	93	439	89
176	350	115	346	97	513	91
192	373	117	361	100	488	93
208	390	118	391	99	504	91
224	403	120	417	102	515	96
240	414	119	418	102	538	97
256	424	119	474	105	547	93
272	443	122	482	105	549	99
288	474	127	486	105	573	96
304	489	123	486	104	591	94
320	503	122	517	110	624	96
336	532	133	536	108	628	101
352	540	135	566	106	623	103
368	606	140	577	110	633	100
384	578	131	583	112	644	97
400	600	141	598	113	666	101
416	658	141	601	112	682	101
432	634	140	636	113	724	102
448	664	140	641	118	745	105
464	675	142	669	119	729	100
480	701	141	678	119	732	106

Table 4.2: Average Effective Amplitude $\overline{A'}$ and Average Movement Time $\overline{MT}$ for each Target Amplitude and Device

Effective Amplitude (A') (pixels)	Movement Time (MT) (ms)	Average Maximum Acceleration (a_{max}) $\left(\frac{pixel}{ms^2}\right)$	Estimated Movement Time (ms) $MT_{est} = \pi\sqrt{A'/a_{max}/2}$	Error
70	86	0.049	84	-2%
90	89	0.059	87	-2%
110	91	0.068	90	-1%
130	96	0.076	92	-4%
150	94	0.088	92	-3%
170	94	0.103	90	-4%
190	97	0.107	93	-4%
210	100	0.112	96	-4%
230	102	0.119	98	-4%
250	106	0.119	102	-4%
270	107	0.128	102	-5%
290	109	0.134	103	-5%
310	110	0.137	106	-4%
330	113	0.141	107	-5%
350	114	0.147	109	-5%
370	115	0.150	110	-4%
390	118	0.155	112	-6%
410	119	0.160	113	-6%
430	122	0.160	115	-5%
450	124	0.163	117	-6%
470	124	0.168	118	-5%
490	125	0.179	116	-7%
510	124	0.185	117	-6%
530	127	0.183	119	-6%
550	132	0.181	122	-7%
570	135	0.180	125	-7%
590	138	0.180	127	-8%
610	141	0.177	131	-7%
630	144	0.172	134	-7%
650	147	0.174	136	-8%
670	148	0.175	138	-7%
690	147	0.179	138	-6%
710	153	0.176	141	-8%
730	153	0.178	142	-7%
750	151	0.189	140	-7%
770	156	0.182	145	-7%
790	155	0.185	145	-7%

Table 4.3: Movement Times and Peak Acceleration values for the Mouse for Effective Amplitude, Estimated movement times were done using equation 5.1, where the computed a_{max} is used in place of Gan and Hoffmann's constant for each effective width.

Effective Amplitude (A') (pixels)	Movement Time (MT) (ms)	Average Maximum Acceleration (a_{max}) $\left(\frac{pixel}{ms^2}\right)$	Estimated Movement Time (ms) $MT_{est} = \pi\sqrt{A'/a_{max}/2}$	Error
70	78	0.057	78	0%
90	80	0.073	78	-3%
110	82	0.082	81	-1%
130	85	0.090	84	0%
150	86	0.102	85	-1%
170	87	0.120	84	-3%
190	88	0.128	86	-3%
210	91	0.141	86	-5%
230	89	0.160	84	-5%
250	91	0.167	86	-6%
270	91	0.182	85	-7%
290	94	0.182	89	-6%
310	93	0.197	88	-5%
330	95	0.203	89	-6%
350	97	0.205	92	-6%
370	98	0.208	94	-5%
390	101	0.213	95	-6%
410	102	0.228	94	-7%
430	104	0.226	97	-6%
450	104	0.235	97	-7%
470	105	0.240	98	-6%
490	107	0.242	100	-7%
510	108	0.250	100	-7%
530	108	0.259	101	-7%
550	110	0.261	102	-7%
570	112	0.259	104	-7%
590	112	0.267	104	-6%
610	115	0.264	107	-7%
630	116	0.268	108	-7%
650	118	0.258	111	-6%
670	118	0.263	112	-5%
690	120	0.263	114	-5%
710	122	0.263	116	-5%
730	125	0.239	123	-1%
750	125	0.257	120	-4%
770	123	0.268	119	-3%
790	126	0.267	121	-4%

Table 4.4: Movement Times and Peak Acceleration values for the Stylus for Effective Amplitude, Estimated movement times were done using equation 5.1, where the computed a_{max} is used in place of Gan and Hoffmann's constant for each effective width.

Effective Amplitude (A') (pixels)	Movement Time (MT) (ms)	Average Maximum Acceleration (a_{max}) $\left(\frac{pixel}{ms^2}\right)$	Estimated Movement Time (ms) $MT_{est} = \pi\sqrt{A'/a_{max}/2}$	Error
70	76	0.064	73	-3%
90	77	0.082	74	-4%
110	77	0.105	72	-7%
130	81	0.113	75	-7%
150	83	0.114	81	-3%
170	86	0.120	84	-3%
190	84	0.140	82	-3%
210	86	0.152	83	-4%
230	86	0.166	83	-4%
250	85	0.181	82	-3%
270	86	0.195	83	-4%
290	85	0.211	82	-3%
310	87	0.215	84	-3%
330	89	0.219	86	-4%
350	88	0.239	85	-3%
370	87	0.258	84	-3%
390	88	0.269	85	-3%
410	89	0.271	86	-3%
430	92	0.272	88	-4%
450	92	0.280	89	-4%
470	93	0.285	90	-3%
490	93	0.296	90	-3%
510	96	0.290	93	-3%
530	95	0.310	92	-3%
550	98	0.299	95	-3%
570	98	0.310	95	-3%
590	98	0.324	95	-4%
610	98	0.334	95	-3%
630	99	0.332	97	-3%
650	99	0.348	96	-3%
670	101	0.347	98	-3%
690	99	0.365	97	-3%
710	101	0.362	98	-2%
730	101	0.370	99	-2%
750	101	0.382	98	-3%
770	103	0.387	99	-4%
790	103	0.383	101	-2%

Table 4.5: Movement Times and Peak Acceleration values for the Isometric Joystick for Effective Amplitude, Estimated movement times were done using equation 5.1, where the computed a_{max} is used in place of Gan and Hoffmann's constant for each effective width.

Table 4.2 shows our movement time results for the three devices and thirty-one target amplitudes. Table 4.1 shows movement time and regression results for each device in our experiment. During analysis, we converted all distance measurements to movement of the hand in cm in the real world, allowing us to compare hand velocity and acceleration between devices. Results indeed suggest a linear relationship between movement time and the target amplitude for all devices.

4.2 Movement Time

Mean movement times for the stylus, mouse, and isometric joystick were 102, 120, and 95 ms respectively. For our main effect, we found a significant difference in movement time between devices ($F_{2,930} = 158.75, p < .001$). Pairwise comparisons showed significant differences between all pairs (after Bonferroni corrections: mouse vs. isometric joystick $p < 0.001$, mouse vs. stylus $p < 0.001$, stylus vs. isometric joystick $p < 0.001$). There was a significant effect of target amplitude ($F_{30,930} = 10.04, p < .001$), but no interaction effect between device and amplitude ($F_{60,930} = 1.06, p = .354$).

4.3 Fit to model of A'

Figure 4.1 shows the scatter plot and regression lines for movement time (MT) versus effective amplitude (A'). Regression shows a best match for a linear relationship between movement time and effective amplitude for all devices, with r2 for

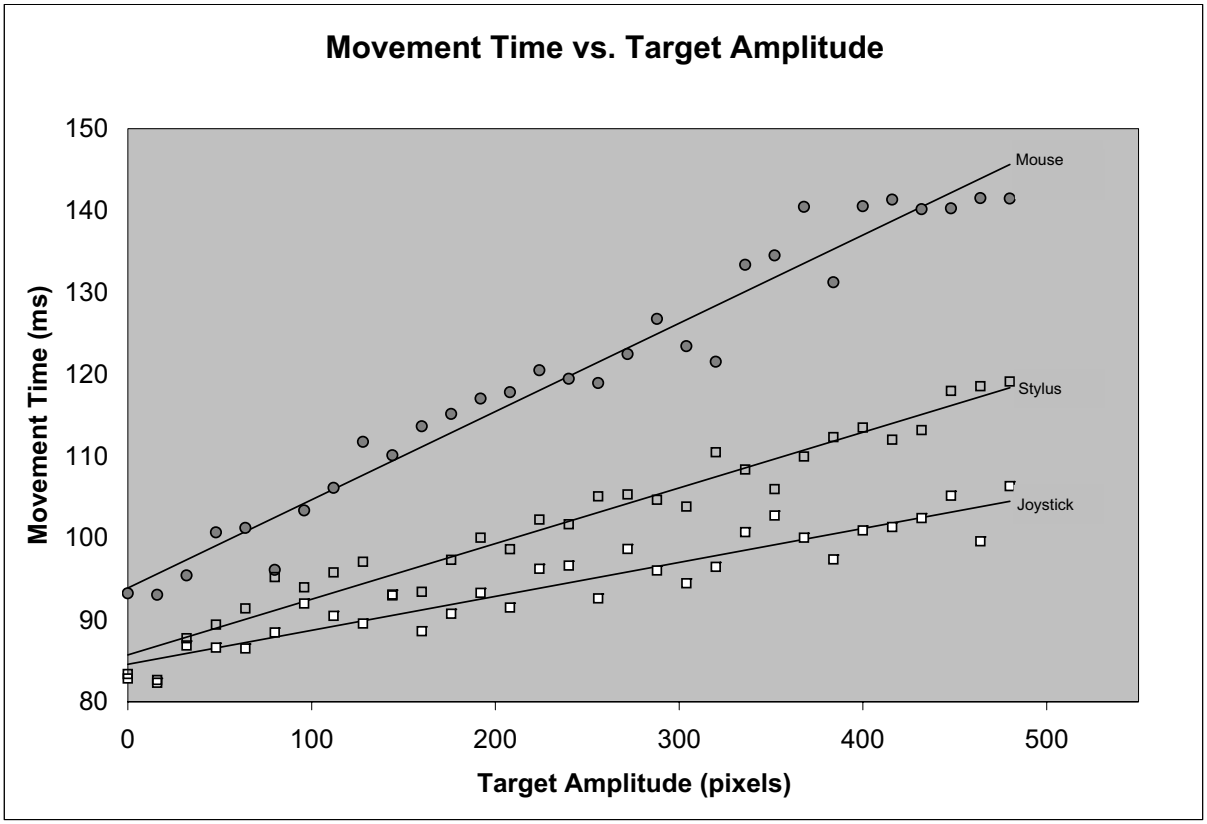

Figure 4.1: Regression lines and scatter plot for movement time versus effective amplitude (A') per device

stylus, mouse and joystick of .99 ($F_{1,36} = 5945.4, p < 0.001$), .99($F_{1,36} = 3894.5, p <$ 0001)and.94($F_{1,36} = 522.5, p < .0001$) respectively.

We also tried to fit a square root model suggested by Gan and Hoffmann. Regression for movement time with the square root of effective amplitude (A') results in a lower r2 for the stylus, mouse of 0.97 ($F_{1,36} = 1302.3, p < .0001$), 0.97($F1, 36 =$ $1112.3, p < .0001$) respectively, with the joystick at 0.96 ($F_{1,36} = 782.7, p < .0001$).

4.4 The Relationship Between A' and A

We now have an expression for movement time in terms of the effective amplitude, which is indeed linear. For predictions, however, a relationship in terms of the target amplitude would be preferred. Figure 4.3 shows the relationship between target amplitude and effective amplitude. From inspection of the graph we see that the effective amplitude for all three devices is quiet linear, and that the effective amplitudes for the mouse and stylus seem to overlap one another. The regression for effective amplitude (A') vs. the target amplitude (A), as suggested, resulted in a very high r2 for the stylus, mouse and joystick of 0.99 ($F_{1,29} = 3555.2, p < .0001$), 0.99($F_{1,29} =$ $4388.3, p < .0001$)and0.97($F_{1,29} = 1181.78p < .0001$) respectively. Because effective amplitude is highly linear with target amplitude and movement time is linar with effective amplitude. It should also be the case that movement time is linear with target amplitude.

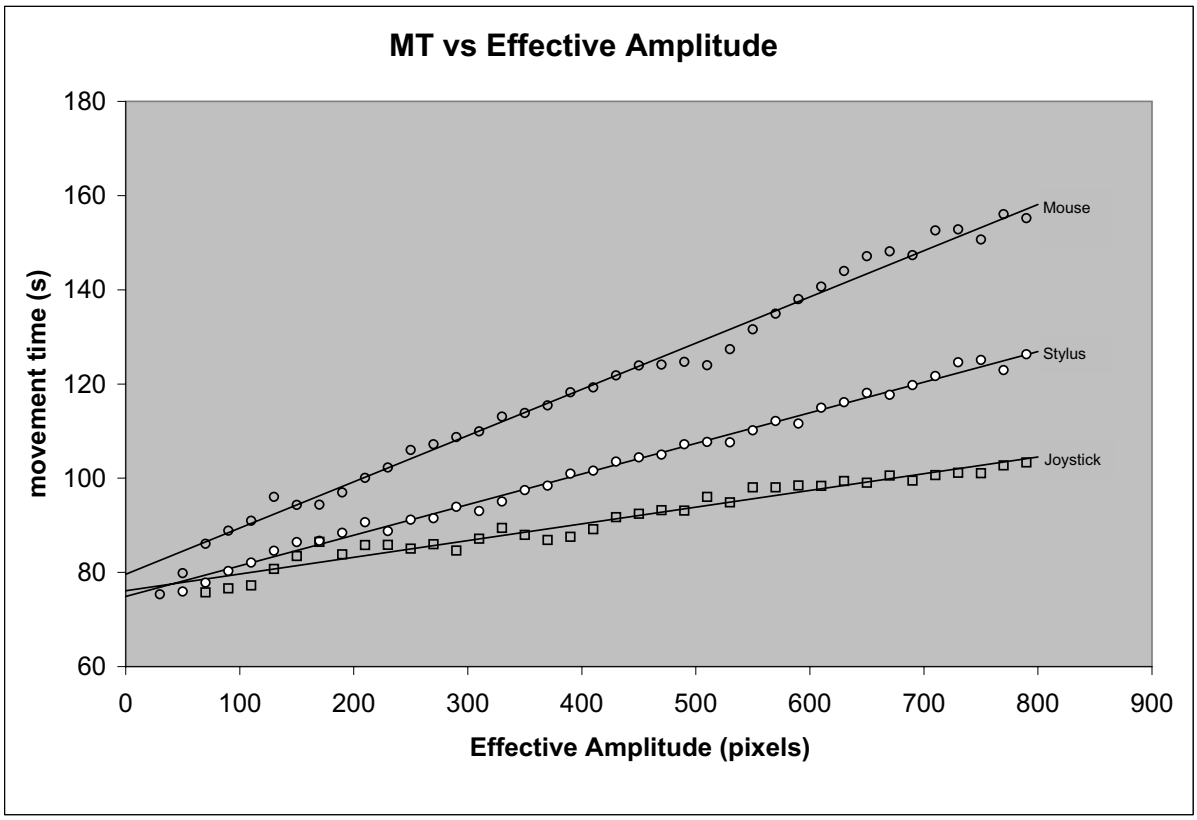

Figure 4.2: Regression lines and scatter plot for movement time versus target amplitude (A) per device

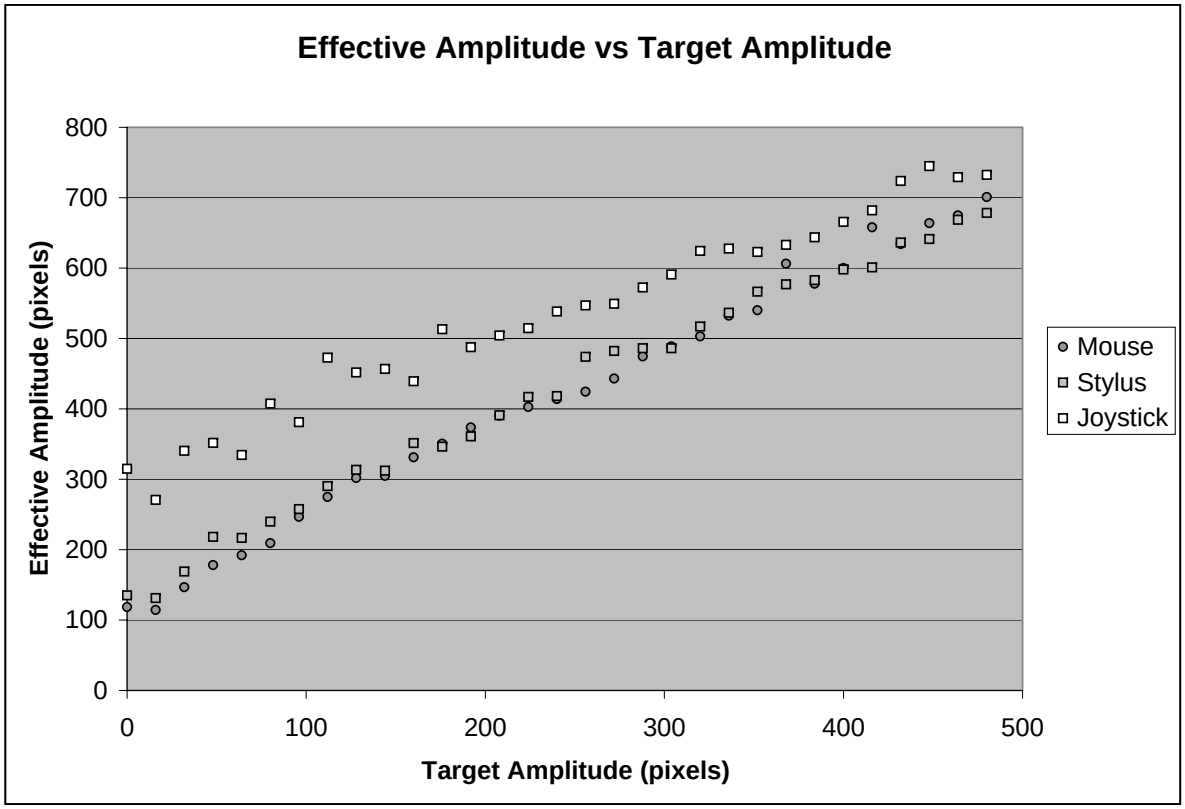

Figure 4.3: Effective Amplitude vs Target Amplitude

4.5 Fit to a Model of A

Figure 4.2 shows the scatter plot and regression lines for movement time (MT) versus target amplitude (A). Table 1 shows the regression coefficients for each device, fit to a model of target amplitude. There were high correlations between movement time and target amplitude for all devices, with an r2 for stylus, mouse and joystick of .96 ($F_{1,29} = 880.0, p < .0001$), .96 ($F_{1,29} = 755.1, p < .0001$), and .89 (($F_{1,29} = 116.7, p < .0001$) respectively. While these correlations were not as high as those for effective amplitude (A'), they are sufficient to more conveniently use A as a predictor of performance. The Index of Performance indicated in 4.1 is the reciprocal of b, and is directly related to the theoretical maximum velocity for each device in this task. For completeness we also examined the fit between movement time and the square root of target amplitude $\sqrt{g}$. Regression showed a lower r2 for stylus, mouse and joystick of .93 ($F_{1,29}$=372.6, $p < .0001$), .92 ($F_{1,29}$=356.1, $p < .0001$), and .87 ($F_{1,29}$=201.6, $p < .0001$) respectively.

4.6 Error Rates

We defined an error as failing to cross the target line after successfully crossing the previous target line. Trails were repeated where subjects obtained greater than 10% error. The average error rate was approximately 5% across all subject-device conditions. Differences between devices were not significant. In traditional Fitts' law experiments, error rates higher than 4% result in a performance/accuracy trade-off that requires adjustment for effective width [16]. Given that our error rate was sufficiently low, and that our purpose was to evaluate performance in cases where target

accuracy constraints were relaxed, we excluded all error cases from analysis. We also designed trials such that each block continued until 50 valid crossings were captured.

4.7 Qualitative Results

After the experiment, we administered a questionnaire that surveyed the participants' qualitative evaluations using Likert-type scales of preference, ease of use, accuracy, and efficiency for each device. Results indicate most participants preferred using the stylus for this task. Preference for the joystick was mixed. Scores for efficiency and accuracy differed significantly between devices: 66% of subjects reported the stylus as most efficient, 33% the joystick and 0% the mouse ($\chi^2 = 8.0, p < .03$). 75% of subjects reported the stylus as most accurate, 25% the joystick and 0% the mouse ($\chi^2 = 10.5, p < .001$).

Many participants also stated that they found the larger amplitude movements extremely demanding on their muscles and joints. We suggest this is because at this large amplitudes the limb is experiencing the maximum force.

Chapter 5

Discussion

5.1 Result summary

Our results show an excellent fit to the simple Hatching law model, one that is better than the fit to Gan and Hoffmann's square root model. In addition, all six regressions resulted in a non-trivial constant component. Gan and Hoffmann's model from Equation 3 does not predict such component. Figure **??** shows the maximum acceleration achieved for the three devices versus effective amplitude, in pixels/ms^2. When units are converted to meters per second squared of real hand movement, we see that the overall maximum acceleration pattern for the stylus levels off at high amplitudes to approximately three times gravity (33 m/s^2), with the mouse levelling off at approximately two times gravity (23 m/s^2). The isometric joystick, however, does not reach an upper limit of maximum acceleration, and remains more or less linear with amplitude. This is most likely because very little actual hand movement is required to operate this device and is consistent with our findings for movement time. For smaller amplitudes, all devices obtained a slower acceleration.

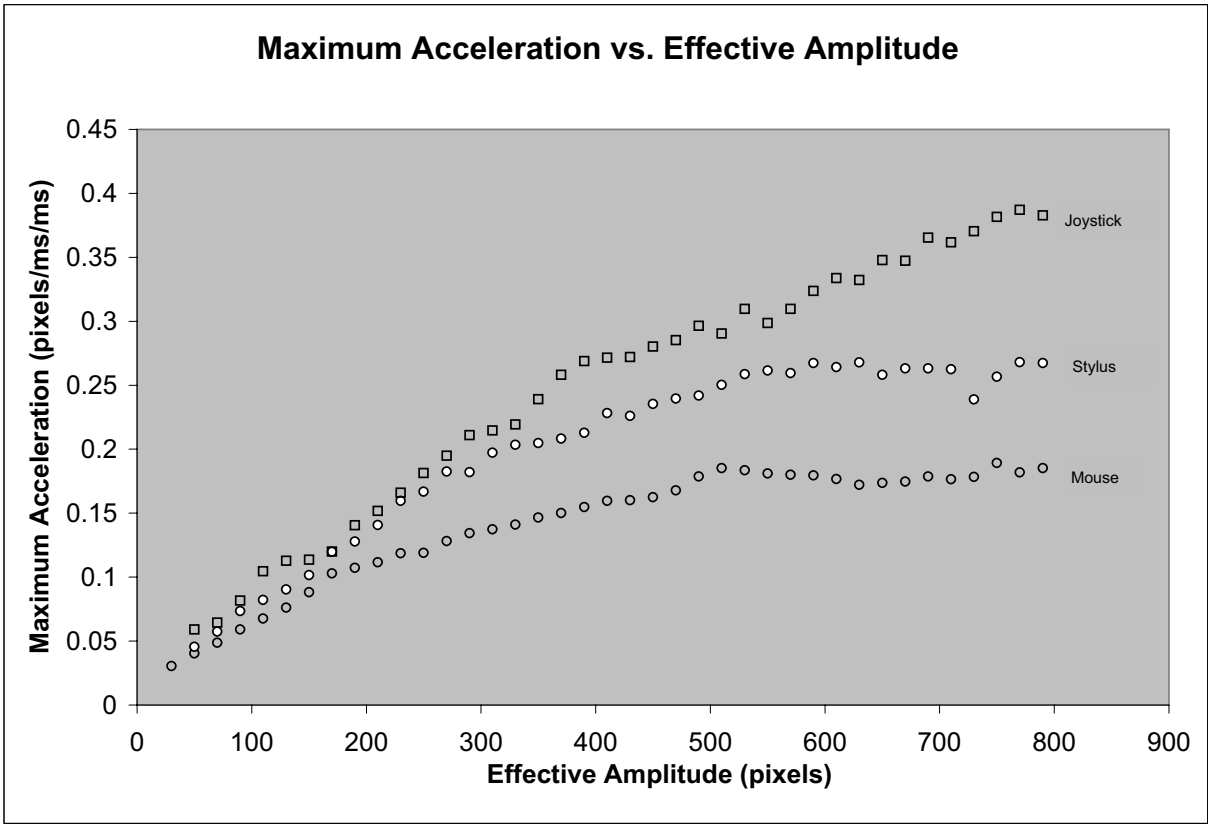

Figure 5.1: Scatter plot of Acceleration versus effective amplitude (A') per device

This contradicts Gan and Hoffmann's assumption that the maximum acceleration is constant, most likely because our target amplitudes were smaller, Gan and Hoffmanns' smallest amplitude was 4cm, this would correspond to a target amplitude of 320 pixels and an effective amplitude of 400 pixels, it this amplitude the maximum acceleration is reached. This means that our results do not contradict Gan and Hoffmanns' result, rather we see that the movement time is linear for these small amplitudes.

Recall that Gan and Hoffmann prediction of movement was given in Equation 1.9 was expressed as in terms of the angular acceleration, if we translate this equation to be in terms of the absolute acceleration of the hand which we compute we get Equation 5.1

$$MT = \sqrt{\frac{\pi^2(A'/2)}{a_{max}}} = \pi\sqrt{\frac{A'}{2a_{max}}} \tag{5.1}$$

, If use our observed maximum acceleration data, the predicted result is within 8% of the observed movement time see tables 4.34.44.5. This means our Hatching law model can be seen as an adaptation of Gan and Hoffmann's model for cases where no clear target width is present. Our model is, however, simpler in that it involves a linear fit.

5.2 The Spring Variable

Figure 5.2 shows the value for the observed spring constants versus effective amplitude for all devices. We computed the value for the spring constant by dividing the maximum acceleration by the extent of the movement, which is half its effective amplitude (A'). When movement time is computed via Equation 1.14, using these empirically obtained values for the spring constant (k), results are within 8% of the actually observed movement times. The spring constant (k) does indeed increase with

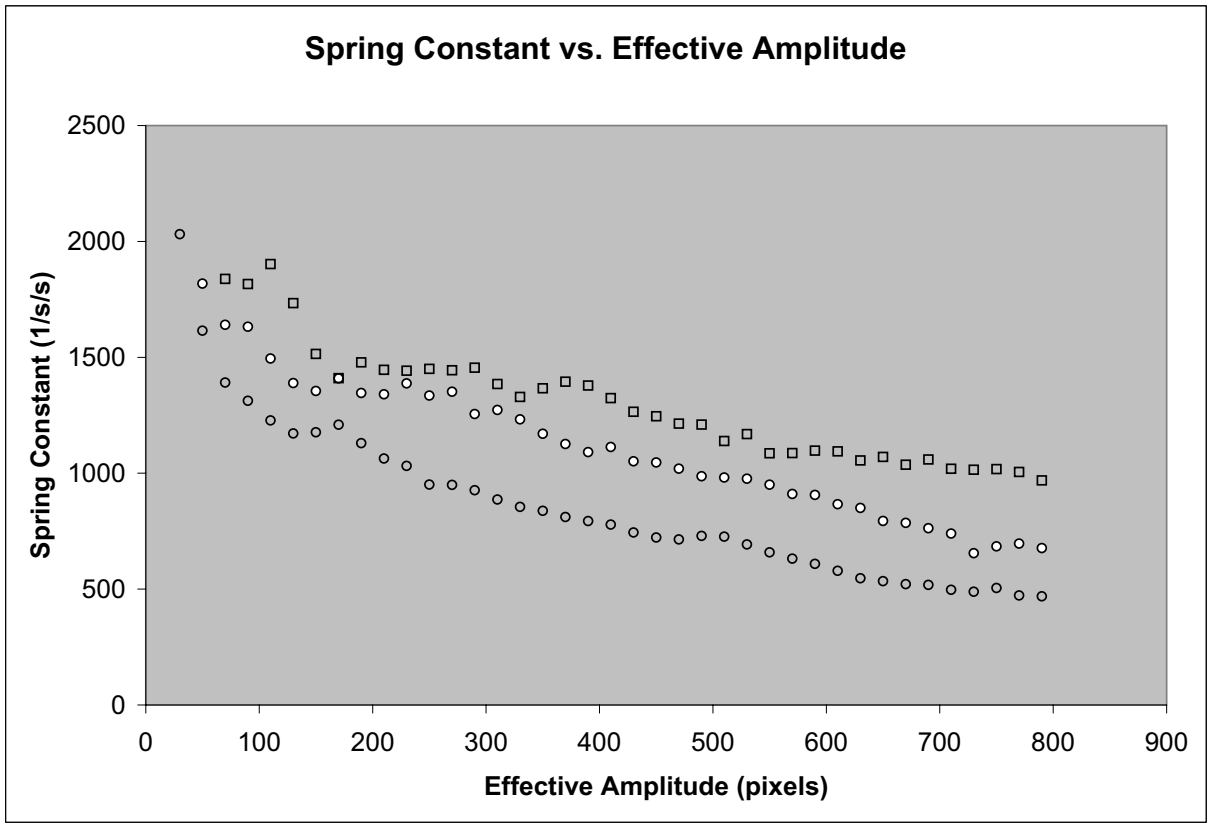

Figure 5.2: Scatter plot of the spring constant versus effective amplitude (A') per device

smaller amplitudes, to a certain limit. It is this limit on k that causes the non-zero constant a in our movement time expression. The y-intercept in the regression in Figure 6 is equal to , where k_{max} represents the maximum stiffness of the limb using each device. It is important to emphasize our task only models the efficiency of oscillatory movements, not their efficacy. We believe that the possible incorporation of curvature control criteria in our task would further underscore our conclusion that the isometric joystick is a very suitable device for these kinds of oscillatory tasks.

5.3 Extending the Hatching Law to Tunneling

In the introduction, we stated that the total movement time for a hatching task was equal to the number of strokes N times the Hatching law. While this is correct for cases where there is minimal movement perpendicular to the strokes, we should correct for cases where the velocity of strokes is limited by that of movement along the tunnel (see Figure 5.3). We can derive a more general form of the Hatching law by incorporating the constraints of moving through a tunnel, as given by the Steering law [2]:

$$MT = a + b\frac{A}{W} \tag{5.2}$$

where a and b are empirically derived constants, and A the length of the tunnel. W constitutes the tunnel width, and is equivalent to A in the original Hatching law (Equation 1.18).

Figure 5.3. Hatching task with movement along a tunnel. Note that W now represents our prior amplitude A. Combining the Hatching law and the Steering law We will now provide a derivation that combines the Hatching law and Steering law in order to describe oscillatory movement through a tunnel. Recall Figure 1b where

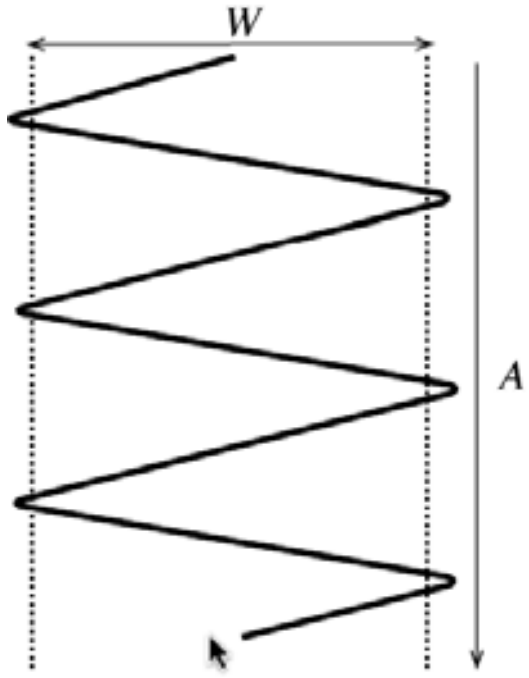

Figure 5.3: Hatching task with movement along a tunnel.

N describes the number of overall strokes. The first step is to recognize that N is equivalent to the number of strokes per distance, n, multiplied by distance A along the tunnel. If we also include a constant h that describes the time to initiate movement, the local form of the Hatching law becomes:

$$MT = An(a + bW) + h \tag{5.3}$$

We will now introduce the effect of steering. The maximum velocity of movement while steering along a tunnel is given by the reciprocal of the steering component in Equation 11, or W/b. To avoid confusion with the b in Equation 12, we will call this W/c instead. The velocity of movement (v_A) along the tunnel will not just depend on the steering component (d). It will also be reduced by the number of strokes per distance, n. This effect is best described as a relative damping of maximum steering velocity by n:

$$v_A = \frac{1}{d}\sqrt{\frac{k}{k+n}} \quad where \quad d = \frac{c}{W} \tag{5.4}$$

k is the damping factor, and an empirically derived constant. Conversely, the velocity of strokes v_w is limited by the velocity of movement along the tunnel, v_A. Again, we obtain a relative damping by n, but now of maximum stroke velocity, given by Equation **??** as 1/b.

$$v_w = \frac{1}{b}\sqrt{1 - \frac{k}{k+n}} \tag{5.5}$$

This is because movement approximates a sawtooth pattern, with the Pythagorean theorem relating both damping factors:

$$1 = \sqrt{(bv_w)^2 + (dv_a)^2} \tag{5.6}$$

This is The reciprocal of v_w, b and the reciprocal of v_A, d provide a description of

movement time:

$$b' = b\sqrt{\frac{n+k}{k}} \tag{5.7}$$

and,

$$d' = d\sqrt{\frac{n+k}{k}} \tag{5.8}$$

Recall $d = \frac{c}{W}$, and for clarity, we define $c' = c\frac{n+k}{k}$. We now expand the local form of the Hatching law in Equation 5.3 by adding a factor describing the time required to stay in the tunnel per stroke: the ID of the Steering law divided by n. The general form of the Hatching law becomes:

$$MT = An\left(a + b'W + \frac{c'}{Wn}\right) + h \tag{5.9}$$

Given our damping factors, we will now prove correctness of the general form of the Hatching law for limiting cases. If n approximates 0, we move along the tunnel, and time is described by the Steering law:

$$\lim_{n \to 0} = A\left(\left(\lim_{n \to \infty} b'n\right)W + \frac{\lim_{n \to 0} c'}{W}\right) + h \tag{5.10}$$

$$\lim_{n \to 0} = h + c\frac{A}{W} \tag{5.11}$$

If n approximates infinity, we stroke in place, and time is described by the local form of the Hatching law:

$$\lim_{n \to \infty} = An\left(a + \left(\lim_{n \to 0} b\right)W + \frac{\lim_{n \to \infty} \frac{c'}{n}}{W}\right) + h \tag{5.12}$$

$$\lim_{n \to infty} = An(a + bW) + h \tag{5.13}$$

In this paper, we only propose the general form of the Hatching law as a likely candidate for describing oscillatory movements through a tunnel, based on our empirical

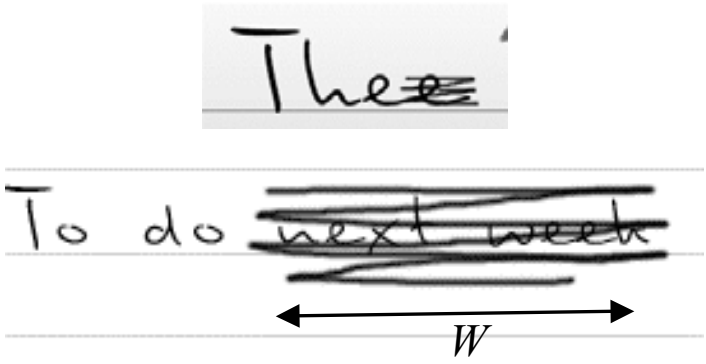

Figure 5.4: Scratching gesture for erasing text on Tablet PCs. Given a constant n and A, movement time is a function of number of letters erased. (*Image courtesy Microsoft cooperation*)

findings with the simple Hatching law. We consider empirical validation of the general form of the Hatching law (Equation 5.9) a future challenge.

5.4 Applications and Future Directions

There are numerous applications of the Hatching law, for example, in graphical tasks that require pen-based input. Modern Tablet PCs facilitate both handwriting and gesture-based input. One example of the application of the Hatching law in such systems lies in the modeling of the scratching gestures used for erasing graphical objects.

Figure 5.4 shows the use of a scratching gesture on a Tablet PC for erasing handwritten characters. Given a constant number of strokes per line, a constant line height and character width, movement time is a function of the number of characters erased. Figure 5.5 shows a corresponding scratching gesture for erasing graphical

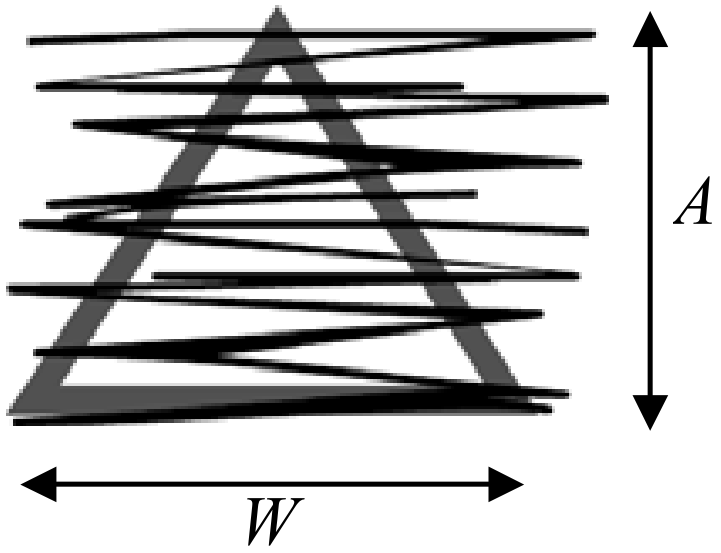

Figure 5.5: Scratching gesture for erasing graphic objects on Tablet PCs. Given a constant n, movement time is a function of the object's overall width and height.

objects. Here, given a constant n, movement time is a function of the area of the bounding box that encloses the object. Modulation Tasks Our results provide clear support for augmenting a stylus with isometric input. Indeed, most tablet styli feature an isometric tip, typically used to control line thickness [26].

Figure 5.6 shows a model of a hatching task where the line thickness is modulated at a given frequency. The trajectory of the line is controlled by movement of the stylus, while line thickness is controlled through pressure exerted on the stylus tip. Movement time in this task should follow the general form of the Hatching law, where W corresponds to the maximum thickness of the line, and A corresponds to the length of the stylus trajectory (given a constant n). We consider the evaluation of this task a future direction.

Figure 5.7 Mimicking isometric vibrato control of the violin in computer music

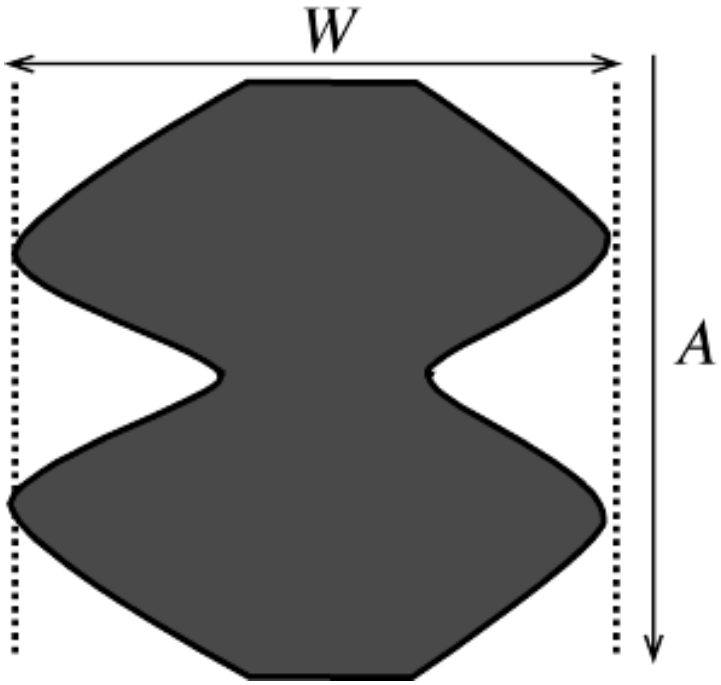

Figure 5.6: Line thickness modulation in a line drawing task

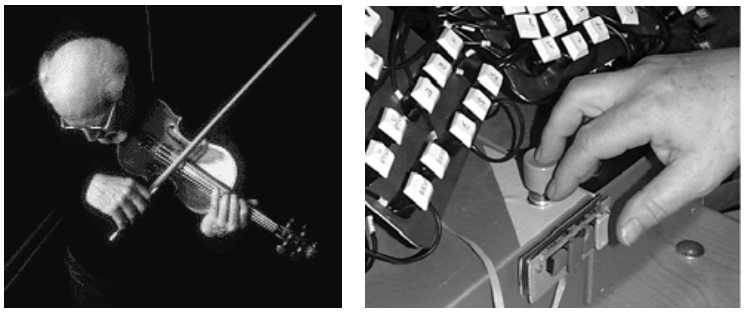

Figure 5.7: Mimicking isometric vibrato control of the violin in computer music instruments such as SenseOrg (right), which features the Sentograph isometric joystrick used in our experiment.

instruments such as SensOrg (right), which features the Sentograph isometric joystick used in our experiment. The visual task shown in Figure 5.7 perhaps corresponds closely to that of vibrato control in musical instruments. Figure 5.7 shows how vibrato control in a violin may be mimicked in a computer music instrument such as SensOrg [25][25] through isometric input. As with the violin, the finger is rocked back and forth without changing position, thus modulating the pitch of the sound. Both Clynes [**?**] as well as Ungvary and Vertegaal [24] argue that isometric devices are inherently better suited for such tasks than isotonic devices. We hope the Hatching law will provide a valuable tool for empirical validation of that claim.

Chapter 6

Conclusion

In this thesis, we presented an adaptation of Gan and Hoffmann's model to describe oscillatory movements that do not aim for a particular target area, such as those found in tasks such as shading, hatching or musical vibrato. Due to their ballistic nature, users' performances in such tasks cannot be adequately modeled with Fitts' law, as applied to pointing tasks. We presented an experimental paradigm for investigating oscillatory tasks based on a simple ballistic hatching task. We found that a simple Hatching law indeed exists, which we used to compare performance of three input devices: stylus, isometric joystick and mouse. Results show a best fit with a linear model, with the isometric joystick outperforming both stylus and mouse. We believe this is because it required the least limb movement. Results also suggest that the spring constant of the hand/arm system is altered to achieve high acceleration at small target amplitudes. However, acceleration with small target amplitudes does not match that of larger target amplitudes.

Bibliography

[1] J. Accot and S. Zhai. Beyond fitts' law: Models for trajectory-based hci tasks.

[2] J. Accot and S. Zhai. Performance evaluation of input devices in trajectory-based tasks: An appicaltion of the steering law. *Proceedings of ACM CHI'99 Conference on Human Factors in Computing Pittsburgh:ACM Press*, pages 466–472, 1999.

[3] J. Accot and S. Zhai. Refining fitts' law models for bivariate pointing. *Proceedings of ACM CHI'03 Conference on Human Factors in Computing Systems Ft. Lauderdale:ACM Press*, NA(NA):73–80, NA 2003. NA.

[4] Kantowitz. B.H. and Elvers. G.c. fitts' law with an isometric controller: Effects of order of control and control-display gain. *Journal of Motor Behavior*, 20:53–66, 1992.

[5] Shannon C. and W. Weaver. *The Mathematical Theory of Communication*. Urbana:University of Illinois Press, 1948.

[6] English W.K. Card, S.K. and B.J. Burr. Evaluation of mouse, rate-controlled isometric jeystick, step keys and text keys for text selection on a crt. *Ergonomics*, 21(8):601–613, 1978.

[7] Clynes. *In Biomedical Engineering Systems*, volume 4, chapter 7: Toward A View of Man. McGraw-Hill, 1970.

[8] E. Crossman. The speed and accuracy of hand movements. Technical report, Report to MRC an DSIR, Joint Committee on Individual Efficiency in Industry (unpublished), 1957.

[9] S.A. Douglas and A.K. Mithal. The effect of reducing homing time on the speed of a finger-controlled isometic pointing devices. *Proceedings of ACM CHI'97 Conference on Human Factors in Computing Boston:ACM Press*, (411-416), 1994.

[10] B.W. Epps. Comparision of six cursor conrol devices based on fitts' law models. *Proceedings of the Annual Meeting of the Human Factors Society*, pages 327–331, 1986.

[11] Hoffmann E.R. and Gan K.C. Directional ballistic movement with transported mass. *Ergonomics*, 31:841–856, 1988.

[12] S. Goldman. *Information Theory*, volume 1 of *3*. New York, Prentice-Hall, 4, 5 edition, 6 1953. 7.

[13] Y. Guiard. Harmonicity in cyclical aiming. *Acta Psychologica (82)*, pages 139–159, 1993.

[14] Gan K.C. and Hoffmann E.R. Geometrical conditions for ballistic and visually controlled movement. *Ergonomics*, 31:829–839, 1988.

[15] Radwin R.G. Lin J.H. and Nembhard D.A. Ergonomics applications of a mechanical model of the human operator in power hand tool operation. *Journal of Occupational and Environmental Hygiene*, 2:111–119, 2005.

[16] I.S. MacKenzie. Fitts' law as a research and design tool in human-computer interaction. *Human Computer Interaction*, 1992:91–139, 7.

[17] I.S. MacKenzie and W. Buzton. Extending fitts's law to two-dimenional tasks. *Proceedings of ACM CHI'92 Conference on Human Factors in Computing Systems. Monterey:ACM Press*, (219-226), 1992.

[18] Sellen A. MacKenzie, I.S. and W. Buxton. A comparison of input devices in elemental pointing and dragging tasks. *Proceedings of ACM CHI'91 Conference on Human Factors in Computing Systems. New Orleans:ACM Press*, (161-166), 1991.

[19] and Douglas S.A. Mithal, A.K. Differences in movement microstructures of the mouse and finger controlled isometric joystick. *Proceedings of ACM CHI'96 Conference on Human Factors in Computing Systems. Vancouver:ACM Press*, pages 114–121, 1996.

[20] Fitts P.M. The informantion capacity of the human motor system in controlling the amplitude of movement. *Journal of Experimental Psychology*, 47:381–391, 1954.

[21] E.C. Poulton. *Tracking Skill and Manual Control*. Academic Press, 1974.

[22] J.D. Rutledge and T. Selker. Force-to-motion functions for pointing. *Proceedings of INTERACT '90, Amsterdam: Elsevier Science*, pages 701–706, 1990.

[23] Zhai S. and P. Milgram. Human performance evaluation of manipulation schemes in virtual environments. *Proceedings of IEEE Virtual Reality Annual International Symposium (VRAIS'93)*, pages 155–161, 1993.

[24] T. Ungvary and R. Vertegaal. Sensorg: Time-complexity and the design of a musical cyberinstrument. *Proceedings of International Computer Music Conference (ICMC'99). Beijing: ICMA*, pages 363–366, 1999.

[25] R. Vertegaal and T. Ungvary. Tangible bits and malleable atoms in the design of computer musical cyberinstrument. *Extended Abstracts of CHI '01 Conference of Human Factors in Computing Systems. Seattle: ACM Press*, pages 311–312, 2001.

[26] Wacom Company Ltd. *Intuos 2 User Manual for Windows V4*, June 2001.

[27] A.T. Welford. *Fundamentals of Skill.* London:Methuen, 1968.